

Experimental Assessment of Feature-based Lidar Odometry and Mapping

Asad Ullah Khan
University of Parma, Italy
Parma, Italy
asadullah.khan@unipr.it

Ernesto Fontana
University of Parma, Italy
Parma, Italy
ernesto.fontana@unipr.it

Dario Lodi Rizzini
University of Parma, Italy
Parma, Italy
dario.lodirizzini@unipr.it

Stefano Caselli
University of Parma, Italy
Parma, Italy
stefano.caselli@unipr.it

Abstract—This paper experimentally evaluates the performance of Lidar Odometry and Mapping (LOAM) algorithms based on two different features namely edges and planar surfaces. This work substitutes the LOAM current feature extraction method with novel SKIP-3D (SKeleton Interest Point 3D) which exploits the sparse Lidar point clouds obtained from 3D Lidar to extract high curvature points in the scan through single point scoring. The prominent features of the proposed method are the detection of sparse, non-uniform 3D point clouds and the ability to produce repeatable key points. Carefully excluding the occluded regions and reduced point cloud after discarding non-significant points enables faster processing. The original F-LOAM feature extractor and SKIP-3D were tested and compared in several benchmark datasets.

Index Terms—Point Cloud, Multi-layer Lidars, Mapping.

I. INTRODUCTION

Multi-layer Lidars have become popular for several applications including autonomous driving and industrial applications. These sensors acquire high range accurate geometric measurements and provide accurate representation of 3D scene occupancy with a single scan in the form of point clouds. Their main limitation lies in non-uniform angular resolution and field-of-view (FoV) of range measurements, which are vertically sparse and horizontally dense. The large amount of data collected is also a challenge for online computations like point set registration, sensor odometry and mapping.

Because of these issues, standard registration methods for mapping like Iterative Closest Point (ICP) [1] or Normal Distribution Transform (NDT) [2] may incur into inaccurate estimation due to wrong association or may perform inefficiently. Specialized algorithms have been proposed for the sparse point clouds acquired by multi-layer Lidars. An effective approach relies on extraction of salient features that facilitates association and registration. LOAM [3] is among the first effective algorithms using crafted keypoints for pairing consecutive points. Several improved versions of the algorithm have been proposed to operate with other sensors. For example, F-LOAM (Fast LOAM) [4] is an efficient and effective system that requires only 3D Lidar measurements. It extends the original work by combining the geometric and images data, working on detection of high curvature points (edge) and planar patches (surface) from point clouds organized in different layers. Other registration and mapping tools such as LIO (Lidar Inertial Odometry) [5] and IN2LAMA (INertial

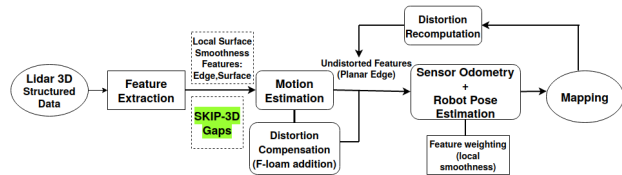


Fig. 1. (F-)LOAM algorithm steps, including SKIP-3D addition

Lidar Localization And Mapping) [6] are based on similar features.

In this paper, we experimentally evaluate the performance of Lidar Odometry and Mapping algorithms based on two different features. The mapping framework consists of the aforementioned F-LOAM combined with F-LOAM original features (*Orig*) and SKIP-3D (SKeleton Interest Point 3D) [7]. The F-LOAM original algorithm computes point saliency according to difference in local neighborhood. Conversely, SKIP-3D finds relevant points through a bottom-up curve simplification procedure that preserves the global shape of each layer. Moreover, SKIP-3D addresses false salient points due to occlusions. The experimental assessment is performed on several benchmark datasets including ICSENS [8], ITU [9] and STEVENS [10].

II. LIDAR ODOMETRY AND MAPPING

Zhang [3] proposed a real-time solution to LOAM by using Lidar odometry to estimate velocity at a higher frequency, while the mapping performs fine processing to create maps at a lower frequency. F-LOAM [4] is presented as an extension of the original LOAM, as it aims to be a lightweight system for estimation of sensor odometry and mapping, willing to use faster computational approaches, specifically while compensating the distortion of previously extracted features.

The Lidar yields a raw point cloud \mathcal{P} . The point cloud is then organized by a property called sweep. A sweep is a 360 degrees rotation that produces a point cloud. As the Velodyne Lidars are collection of different independent lasers (VLP-16, HDL-32, HDL-64), a single scan is collection of points returned by a single laser. Subsequently, the features belonging to successive 3D scans are compared in order to find the optimal transform between two consecutive point clouds.

The Lidar Mapping block repeatedly receives data at 1 Hz from the Lidar Odometry block.

The distortion in LOAM is corrected from one point cloud to another point cloud by comparing and estimating the transformation between them. In opposition to LOAM, the distortion compensation in F-LOAM is double stage distortion compensation, which enables the algorithm to greatly reduce the computational cost. The scanning time between two consecutive Lidar scans is very short, therefore velocities can be considered as constant between two consecutive scans at the first stage, when estimating the motion and correcting the distortion. During the second stage, after pose estimation, the distortion is re-calculated and the corrected features are added to the final map. The pose estimation takes the obtained corrected features after finding the transform between two successive scans and aligns them with global feature map.

For each cluster of neighbor edge points, the algorithm computes a covariance matrix and the edge direction \mathbf{n}_e is equal to the largest eigenvalue of that covariance matrix. Each edge point \mathbf{p}_e is associated to an edge point \mathbf{p}_e^g with its edge direction \mathbf{n}_e^g in the global map (superscript g refers to the reference frame of the global map). Hence, the distance between edge point \mathbf{p}_e and its corresponding global map feature \mathbf{p}_e^g is defined as

$$\mathcal{F}_e(\mathbf{p}_e) = \mathbf{p}_n^\top \cdot ((\mathbf{T}_k \mathbf{p}_e - \mathbf{p}_e^g) \times \mathbf{n}_e^g) \quad (1)$$

where \mathbf{T}_k is the transformation matrix representing the k -th robot pose with respect to the global frame and the unit vector \mathbf{p}_n is given by

$$\mathbf{p}_n = \frac{(\mathbf{T}_k \mathbf{p}_e - \mathbf{p}_e^g) \times \mathbf{n}_e^g}{\|(\mathbf{T}_k \mathbf{p}_e - \mathbf{p}_e^g) \times \mathbf{n}_e^g\|} \quad (2)$$

Similarly, each cluster of surface points \mathbf{p}_s has a covariance matrix and plane norm \mathbf{n}_s corresponding to the eigenvector associated to its smallest eigenvalue. The surface points and plane norm in the global map are labeled respectively as \mathbf{p}_s^g and \mathbf{n}_s^g . The distance between a planar feature \mathbf{p}_s and its associated map feature \mathbf{p}_s^g is equal to

$$\mathcal{F}_s(\mathbf{p}_s) = (\mathbf{T}_k \mathbf{p}_s - \mathbf{p}_s^g)^\top \cdot \mathbf{n}_s^g \quad (3)$$

The transformation \mathbf{T}_k is found by minimizing the sum of the distances of edge and surface features between the current scan and the global map.

When the translational or rotational change is greater than already set threshold, a new keyframe is obtained. Each new keyframe is used to update the global map which consist of edge global map and planar global map.

III. LIDAR FEATURES: CURVATURE-BASED KEYPOINTS AND SKIP

Point clouds acquired by 3D Lidars are sparse and organized in vertical layers. This structure of Lidar data strongly influences the feature algorithms proposed to detect salient regions in data. The input points are often partitioned into layers that can be processed independently. The underlying assumption is that the points of a layer are samples of a continuous curve.

TABLE I
AVERAGE TRANSLATIONAL DIFFERENCE (ATD) AND AVERAGE ROTATIONAL DIFFERENCE (ARD) OBTAINED BY F-LOAM WITH FEATURES *skip* W.R.T. FEATURES *orig*.

Dataset	ATD [%]	ARD [$10^{-2^\circ}/m$]	Step [m]
ICSENS 01	1.691	1.025	100
ICSENS 02	0.974	1.133	100
ICSENS 03	3.563	1.984	100
ICSENS 04	1.548	0.9971	100
ICSENS 05	1.681	1.064	100
ICSENS 06	1.600	1.369	100
ICSENS 07	1.099	0.698	100
ICSENS 08	1.226	0.7573	100
ITU 01	11.600	15.288	100
ITU 02	9.662	8.863	60
ITU 03	4.963	8.586	20
STEVENS 01	4.783	6.694	40
STEVENS 02	21.178	25.276	40
STEVENS 03	4.159	4.770	40

Inside each layer the points are sufficiently dense for shape description and, moreover, can be radially sorted.

F-LOAM exploits layer-based processing to detect points in high curvature and flat regions. The former are found by thresholding a smoothness parameter computed on a sliding window interval of $2w + 1$ beams (with fixed $w = 5$). Let $\mathcal{P} = \{\mathbf{p}_i\}_{i=0, \dots, n_l-1}$ be the points of one layer (the layer index is omitted for simplicity). The smoothness of a point \mathbf{p}_i is defined as

$$\sigma_i = \frac{1}{2w} \sum_{j=-w}^w \|\mathbf{p}_{i+j} - \mathbf{p}_i\| \quad (4)$$

The classification of points according to their σ_i is performed on a section of $n_l/6$ consecutive measurements. The points with σ_i greater than a threshold (set to 0.1) are marked, but only the first 20 with largest curvature in the sector are labeled as edges. The unmarked points are classified as surfaces.

This smoothness parameter used to discriminate features has several disadvantages. First, its value depends only on the relative distance between the point and its neighbors, without taking into account the global shape of the layer. Second, it overlooks that high values of σ_i may be caused by occlusions or other sensor limitations rather than high curvature. The proposed SKIP-3D algorithm [7] addresses these issues. SKIP-3D also operates on layers and searches for salient points, but it implements additional criteria. First, the sequences of points in a layer are split in correspondence to gaps which are due to occlusions. The salient point detection is inspired by the bottom-up polyline simplification algorithm proposed in [11]. Each point \mathbf{p}_i , except for invalid ranges or gap points, has a previous and next point, respectively \mathbf{p}_{p_i} and \mathbf{p}_{n_i} , according to the radial order holding in each Lidar layer. The saliency of a measurement/point is given by a score. The *cornerness score* of each point is defined as

$$\kappa_i = \|\mathbf{p}_{n_i} - \mathbf{p}_i\| + \|\mathbf{p}_i - \mathbf{p}_{p_i}\| - \|\mathbf{p}_{n_i} - \mathbf{p}_{p_i}\| \quad (5)$$

SKIP points are estimated by iteratively removing the points with lowest values of cornerness κ_i . Every time a point \mathbf{p}_i is

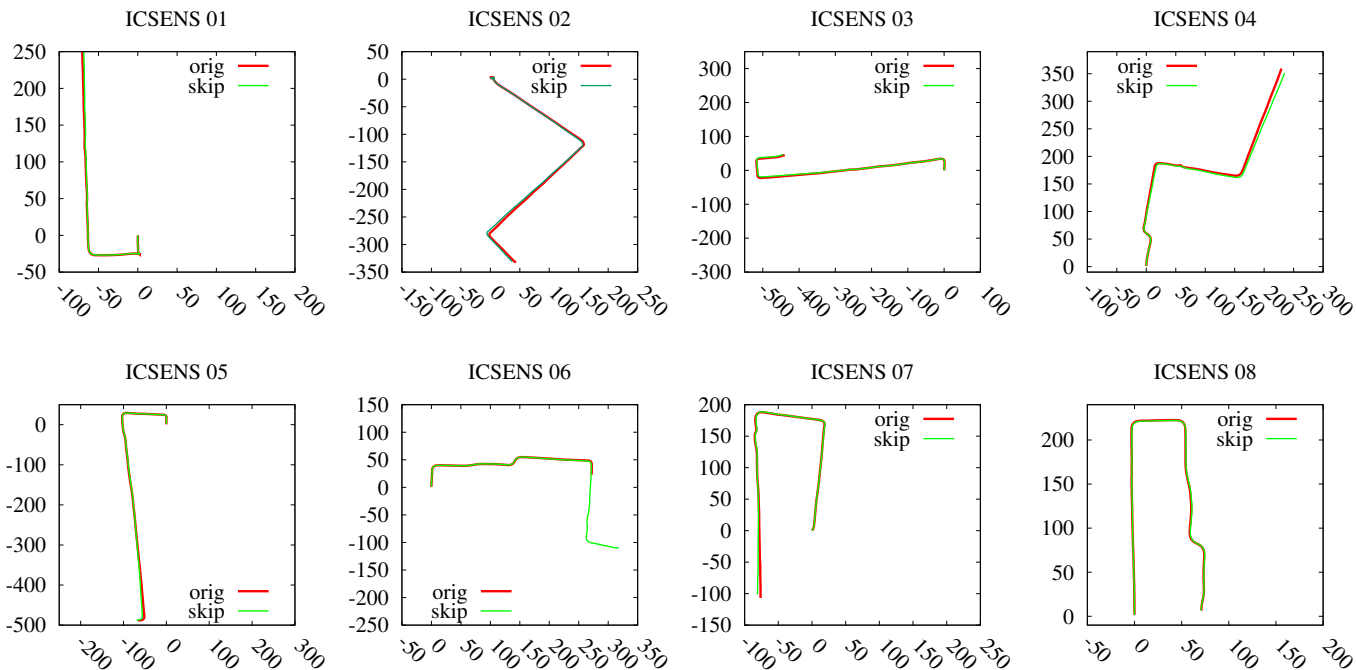


Fig. 2. Robot trajectories estimated using F-LOAM with Original (red) and SKIP features (green) for the *i.c.sens* Visual-Inertial-Lidar Dataset sequences 01-04 (top from left to right) and 05-08 (bottom from left to right). Distances are measured in meters.

removed from a particular ring, its previous and next points \mathbf{p}_{p_i} and \mathbf{p}_{n_i} respectively change. At this stage the score is re-calculated in order to put back related consecutive points. The cornerness values evolve during the procedure and are less and less dependent from local neighborhood. Thus, the remaining points at the end of the procedure provide a faithful representation of global shape. SKIP provides upper hand by distinguishing from original F-LOAM as it maintains the global shape of each layer.

The edge points correspond to the SKIP points computed as described above. The points \mathbf{p}_i are classified as surface if the following conditions hold:

- 1) the radial index i of \mathbf{p}_i belongs to an interval $f \leq i \leq l$ where $\mathbf{p}_f, \mathbf{p}_l$ are either edge points or gaps;
- 2) the distance between \mathbf{p}_i and segment $\overline{\mathbf{p}_f \mathbf{p}_l}$ is less than a threshold s_{th} ;
- 3) the number of points \mathbf{p}_i satisfying the previous conditions on interval $[f, l]$ is greater than a threshold s_{num} .

In summary, surface patches consist of a sufficiently numerous sequence of smooth (aligned) points between two salient points. The classification achieved by F-LOAM original features and SKIP is homogeneous, but the criteria to compute edges and surfaces are significantly different.

IV. EXPERIMENTS

In this section we describe a set of experiments designed to compare the trajectory estimated by F-LOAM when using the proposed SKIP-3D and exploit the high-curvature features. The tests were conducted on the datasets labeled as ICSENS, ITU and STEVENS that are described in the following.

- 1) **ICSENS**. The *i.c.sens* Visual-Inertial-Lidar [8]¹ is provided by a group from the University of Hannover. It has been acquired using Velodyne HDL-64 Lidar (64 layers, vertical resolution 0.5°) at 10 Hz rate. The sensor is mounted on a car vehicle with axis x facing forward driving direction, axis y toward left and axis z upward. The eight sequences labeled as ICSENS-01/08 are result of a 15 minute drive.
- 2) **ITU**. The ITU dataset [9]² provided by Istanbul Technical University is collected using a Husky A200 mobile robot equipped with a Velodyne VLP-16 Puck (16 layers, vertical resolution 2°). The ground vehicle traveled in between trees for about 174 meters to record the data. We used the first 3 sequences of this dataset.
- 3) **STEVENS**. The Stevens-VLP16 dataset [10] provided by Stevens Institute of Technology is collected using a Clearpath Jackal robot equipped with a Velodyne VLP-16 Puck. The robot has been manually guided on a setting consisting of buildings, trees, roads and sidewalks. We used 3 sequences acquired on June 15th 2017³.

Figure 4(a)-(b) displays the maps in the form of point clouds obtained with F-LOAM + SKIP-3D respectively from datasets ICSENS-01 and ICSENS-02. We have computed the paths estimated by F-LOAM with either its original features (hence labeled as *orig* and plotted in red color) and the proposed

¹<https://data.uni-hannover.de/dataset/i-c-sens-visual-inertial-lidar-dataset>

²<https://doi.org/10.25835/0026408>

³<https://tinyurl.com/2p87t9w2>

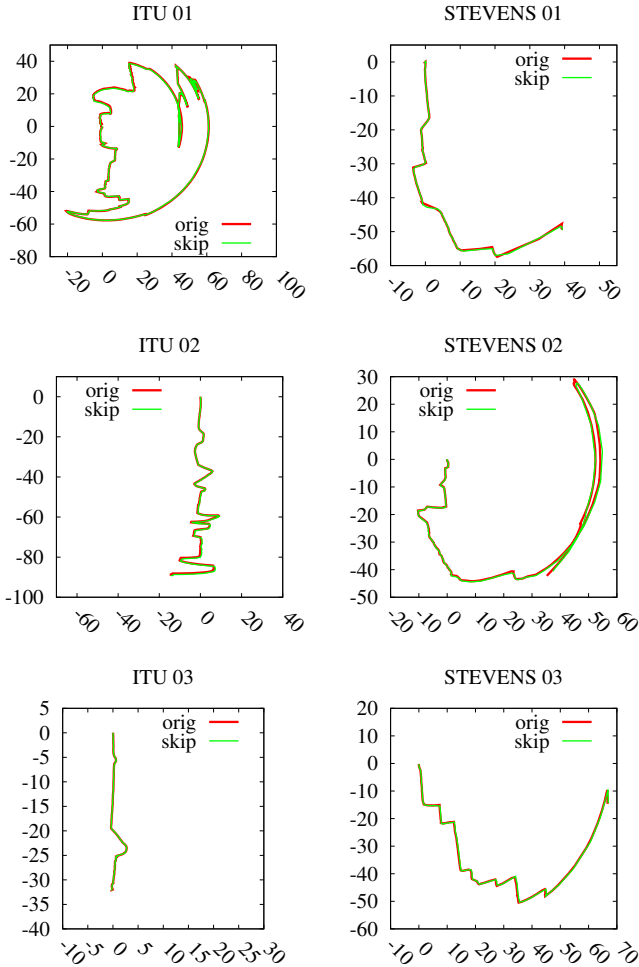


Fig. 3. Robot trajectories estimated using F-LOAM with Original (red), SKIP features (green) for the ITU sequences 01-03 (left) and STEVENS sequences 01-03 (right). Distances are measured in meters.

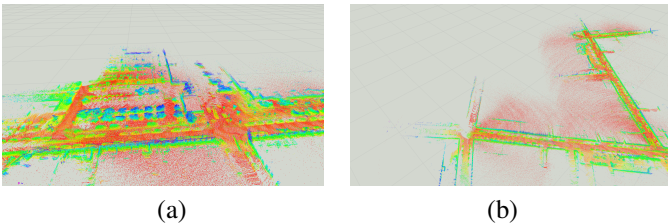


Fig. 4. Complete maps of (a) ICSENS-01 and (b) ICSENS-02 datasets estimated using F-LOAM and SKIP-3D

SKIP-3D (hence labeled as *skip* and plotted in green color). In [7] a significantly smaller ATE and ARE is achieved with SKIP-3D on KITTI dataset. Figures 2 and 3 show the outcomes on datasets ICSENS, ITU and STEVENS. In most cases the paths estimated with *orig* and *skip* largely overlap. An exception is obtained for ICSENS-06 (Figure 2) where the path estimated with *orig* breaks up ahead of time and a failure of *orig* is observed. In the STEVENS dataset the environment varies to better assess the performance of features

extraction algorithm namely Edges and Planar surfaces. In these sequences, the points are returned from tree leaves, which are not stable features in the edge features. However, as the robot moves to the building area features become more clear and consistent in the *skip* by adjusting the threshold. Table I reports the ATD (average translational difference) and ARD (average rotational difference) obtained from *orig* and *skip* which point to discrepancies in the estimated paths. In particular, higher ATD and ARD have been noticed with ICSENS-03, ITU-01 and STEVENS-02 which are evident from the subfigures in Figure 2 and Figure 3 as the *orig* and *skip* slightly diverge.

V. CONCLUSION

In this work, we addressed the inclusion of a novel SKIP-3D for Lidars with F-LOAM in sensor odometry system to assess experimentally the performance of LOAM algorithm. The proposed solution is flexible as it removes non-significant points from each ring of the acquired point cloud while maintaining the global shape of the scan. Experimental results with distinct datasets from dissimilar scenes suggest that SKIP-3D validly extracts features from the Lidar scan. It is expected that the extracted features can be used in future researches to evaluate and monitor the surroundings with the addition of other features.

REFERENCES

- [1] J. Serafin and G. Grisetti, "Using extended measurements and scene merging for efficient and robust point cloud registration," *RAS*, vol. 92, pp. 91–106, 2017.
- [2] M. Magnusson, A. Lilienthal, and T. Duckett, "Scan registration for autonomous mining vehicles using 3d-ndt," *Journal of Field Robotics*, vol. 24, no. 10, pp. 803–827, 2007.
- [3] J. Zhang and S. S. Singh, "LOAM : Lidar Odometry and Mapping in Real-time," in *Proc. of Robotics: Science and Systems (RSS)*, 2014.
- [4] H. Wang, C. Wang, C. Chen, and L. Xie, "F-loam : Fast lidar odometry and mapping," in *Proc. of the IEEE/RSJ Int. Conf. on Intelligent Robots and Systems (IROS)*, no. 3, 2021, arXiv:2107.00822.
- [5] H. Ye, Y. Chen, and M. Liu, "Tightly Coupled 3D Lidar Inertial Odometry and Mapping," in *Proc. of the IEEE Int. Conf. on Robotics & Automation (ICRA)*, 2019, pp. 3144–3150.
- [6] C. L. Gentil, T. Vidal-Calleja, and S. Huang, "In2lama: Inertial lidar localisation and mapping," in *Proc. of the IEEE Int. Conf. on Robotics & Automation (ICRA)*, May 2019, pp. 6388–6394.
- [7] A. Khan and D. Lodi Rizzini, "Novel SKIP Features for LIDAR Odometry and Mappings," in *Proc. of the Int. Conf. on Intelligent Computer Communication and Processing (ICCP)*, Oct. 2021, pp. 1–6.
- [8] R. Voges and B. Wagner, "Timestamp offset calibration for an imu-camera system under interval uncertainty," in *Proc. of the IEEE/RSJ Int. Conf. on Intelligent Robots and Systems (IROS)*, 2018, pp. 377–384.
- [9] A. Aybakan, G. Haddeler, M. Caner Akay, O. Ervan, and H. Temeltas, "A 3d lidar dataset of itu heterogeneous robot team," in *Proc. of Int. Conf. on Robotics and Artificial Intelligence (ICRAI)*, Nov 2019, pp. 12–17.
- [10] T. Shan and B. Englot, "LeGO-LOAM: Lightweight and Ground-Optimized Lidar Odometry and Mapping on Variable Terrain," in *Proc. of the IEEE/RSJ Int. Conf. on Intelligent Robots and Systems (IROS)*, 2018, pp. 4758–4765.
- [11] L. Latecki and R. Lakamper, "Shape similarity measure based on correspondence of visual parts," *IEEE Trans. on Pattern Analysis and Machine Intelligence*, vol. 22, no. 10, pp. 1185–1190, Oct 2000.